Intensity dependence of the multielectron dissociative ionization of N_2 at 305 and 610 nm

C. Cornaggia, J. Lavancier, D. Normand, J. Morellec, and H. X. Liu
Service de Physique des Atomes et des Surfaces, Centre d'Etudes Nucléaires de Saclay, 91191 Gif-sur-Yvette CEDEX, France
(Received 1 May 1990)

We have studied the laser intensity dependence of the multielectron ionization of N_2 in the range of $10^{13}-5\times10^{15}$ W/cm^2 (laser wavelength 305 and 610 nm; pulse duration 2 ps). At 610 nm, we detect four charge states of atomic fragments (N^+, N^{2+}, N^{3+}, and N^{4+}). The fragment kinetic energies and population intensity dependences indicate that they are produced by a sequential ionization occurring during the dissociation of the molecular ions (from N_2^{2+} to N_2^{8+}) and/or formed by subsequent atomic ionization. In the first case our findings imply that the ionization occurs at well-defined internuclear distances. Moreover, the initial kinetic energies of the fragments are independent of the laser intensity. The results are interpreted in terms of laser-pulse development and volume effects. At 305 nm the dissociation processes show a different tendency. We detect two charge states of nitrogen fragments (N^+ and N^{2+}) arising from a vertical excitation of the N_2 molecules.

I. INTRODUCTION

With the advent of powerful lasers, the study of small diatomic molecules irradiated by intense radiation fields has become the subject of growing interest. The interaction processes are described by theoretical treatments involving nonperturbative calculations based on the dressed-state model[1] and applied to the search of high-intensity effects in the molecular photodissociation.[2-5] Experimentally, the high-intensity regime has been studied mainly on atoms. However, the specificity of the molecular structure appears in the above-threshold ionization spectra of H_2 (Refs. 6–8) and N_2 (Ref. 9), where the excess energy of ionization is partitioned between the outgoing electron and the molecular ion populated in different rovibrational levels.

At higher intensity (10^{16} W/cm^2) the interaction of N_2 molecules with subpicosecond pulses has led to the production of multicharged fragments whose formation processes depend on the laser parameters. At a wavelength of 248 nm,[10] the kinetic-energy distributions of ionic fragments present many similarities with those obtained by soft-x-ray excitation where the creation of a core hole leaves the molecule in a highly excited state which decays by Auger cascade. Moreover, it appears that the dynamics favors the dissociation channels leading to an asymmetry in the charge states of the atomic fragments. This is interpreted as a consequence of a large dipole moment arising from the multielectron motion along the laser E field. Another experiment, carried out at 600 nm, leads to a different tendency.[11] First, the results show that the charge symmetric dissociation channels (e.g., $N_2^{4+} \rightarrow N^{2+}+N^{2+}$) are favored at this wavelength. Second, the measured energies are consistent with a sequential ionization mechanism interpreted by a field-ionization Coulomb explosion model.[12]

These results highlight the high sensitivity of the interaction processes with respect to the laser characteristics. Thus, we have studied the multielectron ionization of the N_2 molecule when irradiated by intense picosecond laser radiation. In order to understand the dynamics of the interaction process, we measure the kinetic energies of the dissociation products and study the ion-yield dependence on the laser intensity in the range of 10^{13} to 5×10^{15} W/cm.[2] To investigate the role of the laser wavelength, the experiment is repeated at 610 and 305 nm. The results are presented in Secs. III and IV, respectively, after the description of the experimental setup given in Sec. II. The conclusion is given in Sec. V.

II. EXPERIMENTAL SETUP

A. Laser system

The laser oscillator is a synchropumped Spectra Physics 3500 dye laser operated with rhodamin 6G. At the wavelength of 610 nm, the pulse duration is 2 ps (controlled by a scanning autocorrelator) and the pulse energy is a few nJ.

The amplification is carried out through a four-stage dye amplifier pumped by a Quantel neodymium–yttrium aluminum garnet (YAG) laser delivering 200 mJ at 532 nm with a 10-Hz repetition rate. The first three amplifiers are transversely pumped prism dye cells[3] which allow a homogeneous pumping of the flowing dye and a good spatial quality of the amplified beam. The fourth amplifier is longitudinally pumped. The first amplifier stage is operated with kiton red while the three others are used with rhodamin 640.[14] The solvent is a 2% aqueous solution of ammonix LO.

A saturable absorber jet (malachite green in ethylene glycol) isolates the first two amplifier stages. The amplified stimulated emission (ASE) is at most 60 μJ against 2 mJ for the laser-pulse energy. The time duration of the ASE being 4.5 ns, the laser and ASE power ratio is about 10^5. Thus the contribution of the ASE is

completely negligible in the highly nonlinear processes involved in this experiment.

The laser-pulse duration after amplification is measured using second-harmonic generation and single-shot autocorrelation techniques.[15] Assuming a Gaussian intensity profile, we have found a value of 2 ps. Two different lenses have been alternatively used to focus the laser beam. The former is a spheroparabolic lens of 60-mm focal length which focuses the laser light on a near diffraction-limited focal section of 2.2×10^{-7} cm^2 at 610 nm and 7.8×10^{-7} cm^2 at 305 nm. The latter has a focal length of 150 mm and focuses the laser beam on a spot section of 1.3×10^{-6} cm^2 at 610 nm. The laser-beam-section measurements are performed by analyzing the interaction volume with a videocamera connected to a computer.[16]

For the 305-nm experiment, the laser frequency is doubled using a BBO crystal with a conversion efficiency of 15%. We have verified that the phase-matched bandwidth of the BBO crystal exceeds the bandwidth of the incident 610-nm radiation. Consequently, we obtain a coherent Fourier-transform laser pulse at 305 nm, with a duration of 1.4 ps taken reasonably $\sqrt{2}$ smaller than the laser-pulse duration at 610 nm.

B. Ion time-of-flight analysis

The time-of-flight (TOF) spectrometer is essentially composed of a double field acceleration region,[17,18] a drift tube, and a conventional electron multiplier. In the interaction region, we apply a uniform electric field whose intensity is adapted to the experimental parameter to be measured. (i) To study the relative abundances of the different ion species, the collection electric field is set to 700 V/cm. The ions of each species are gathered into a single peak whatever their initial kinetic energies. (ii) Conversely, to determine the ion kinetic energies, the electric field is varied between 25 and 70 V/cm which ensures a good energy resolution. The field in the accelerating region (defined by two parallel high transparency grids) is stronger and parallelizes the ion trajectories. The ions travel through an 18-cm-long drift tube and are finally accelerated to a few keV on the cathode of the electron multiplier. The ion signals are fed to a Lecroy 100 MHz transient digitizer and finally computer discriminated as a function of the laser-pulse energy.

The vacuum chamber is evacuated by a turbopump coupled to a diffusion pump which works as a booster and significantly improves the pumping speed for light gases. Thanks to periodic moderate outgassings of the chamber, the background pressure can be maintained at about 10^{-9} Torr.

III. STUDY AT 610 nm

A. Results

We show on Fig. 1 a typical TOF ion-mass spectrum recorded at 5×10^{15} W/cm^2 with a 700 V/cm collection electric field. We observe that the dissociation of the nitrogen molecules leads to the formation of multiply charged ions: N^+, N^{2+}, N^{3+}, and N^{4+}. The relative

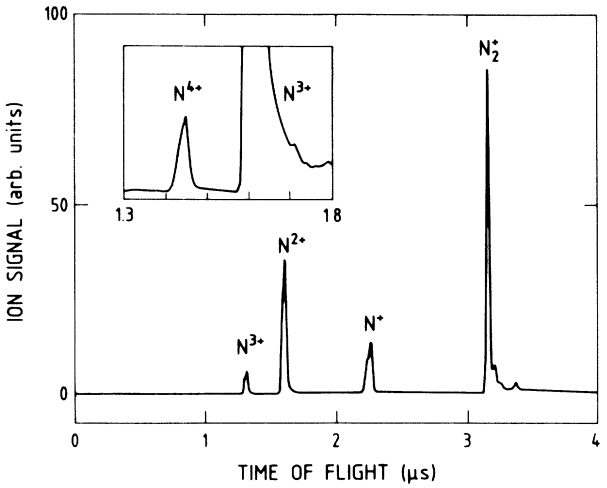

FIG. 1. TOF ion-mass spectrum of N_2 obtained at 5×10^{15} W/cm^2 with a 610-nm, 2ps laser radiation. The pressure in the interaction region is 3×10^{-8} Torr and the extraction field is 700 V/cm. The top left window shows part of another TOF spectrum recorded at 1.4×10^{-6} Torr. The ratio between the N^{3+} and N^{4+} populations is about 50.

abundances of these ions are not corrected for the secondary emission factor of the CuBeO cathode of the electron multiplier, these data being not available in the literature. In fact these correction factors have essentially been measured for the noble-gas ions[19] showing that, in the ion-energy range of a few KeV, the electron multiplier gain should be proportional to the charge state Z of the ion. If we extrapolate the results for rare gases, the ion signals for N^{2+}, N^{3+}, and N^{4+} should be respectively multiplied by the factor $\frac{1}{2}$, $\frac{1}{3}$, and $\frac{1}{4}$, the N^+ ion signal being the reference.

In order to measure the initial kinetic energies of the fragments, we set the extraction field to 50 V/cm which yields the typical TOF ion-mass spectrum represented on Fig. 2(a), recorded with the laser polarization lying along the axis of detection. We note that for each ion species the signals are split into two symmetric components. The "toward" component in the TOF scale is marked by the letter t as it is related to the creation of fragments with an initial momentum directed towards the detector. The "backward" one is noted b as it represents fragments initially headed in the opposite direction and whose momentum has been reversed by the extraction electric field. The time interval Δt separating two associated peaks makes it possible to determine the initial kinetic energy E_0 of the fragments according to the relation:

$$E_0(\text{eV})=Z^2eF^2\Delta t^2/8M \ , \tag{1}$$

in which e denotes the electron charge and F the electric field in the interaction chamber.

To show the structures in detail, the ion signals for N^+, N^{2+}, and N^{3+} are enlarged on Figs. 2(b)–2(d), respectively. We observe that some structures appear in the peaks, corresponding to ions with the same charge

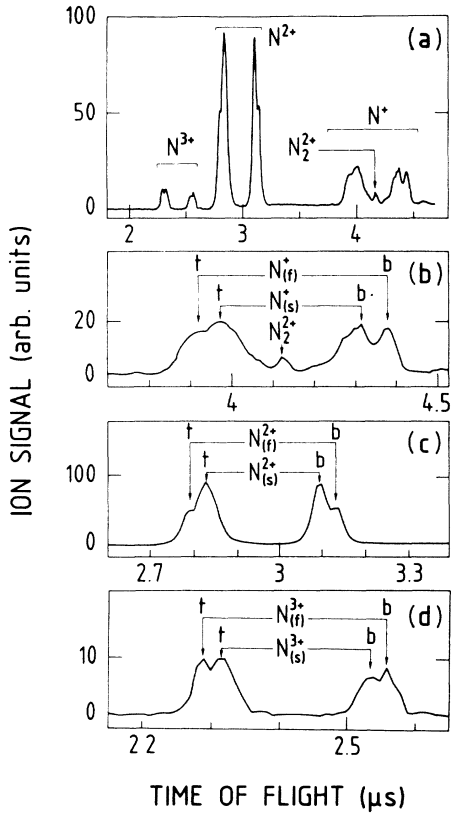

FIG. 2. (a)–(d): TOF ion-mass spectrum of N_2 recorded at 5×10^{15} W/cm^2 and an operating pressure of 2×10^{-7} Torr (which makes it possible to avoid the space charge). A small extraction field of 50 V/cm is applied in order to distinguish the different classes of velocities for each group of atomic ions: (a) complete spectrum, (b)–(d) enlarged views of N^+ -N^{2+}- and N^{3+}-ion signals.

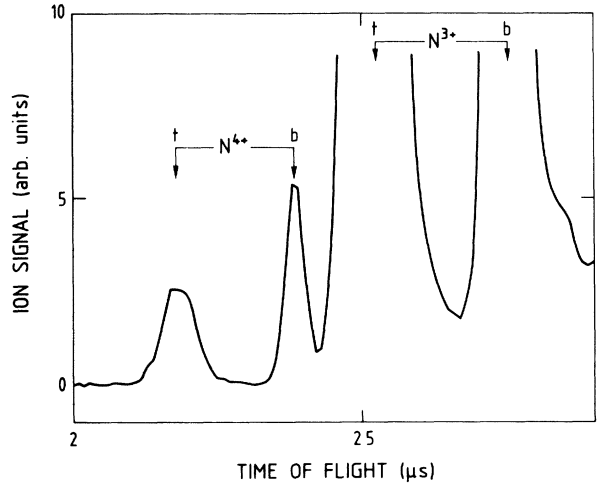

FIG. 3. Enlarged view of N^{4+} signal recorded at 5×10^{15} W/cm^2 and a pressure of 10^{-6} Torr. The asymmetry between the backward and toward peaks is related to the choice of the voltages on the double chamber grids necessary to avoid the overlap between the N^{3+} and N^{4+} ions. The extraction field in the interaction region is 57 V/cm.

and mass but with different kinetic energies. Since for each species, two different energies are identified, we use the s and f subscripts to denote the slow and fast ion classes. The detection and energy analysis of the N^{4+}-ion peak require specific conditions so that it is presented separately on Fig. 3.

The Δt measurements are limited by the digitizer electronic width of 8 ns and can be perturbed by the space charge. Thus, we have also studied the variation of E_0 with the operating pressure (Fig. 4). It appears clearly that the space charge increases the initial kinetic energies of the ions as well as the widths of the peaks. Indeed, after the escape of the electrons, ions located at the periphery of the focal spot are submitted to a repulsive electrostatic force depending on the number of ions in the focal region and thus receive an additional energy. So, we have chosen operating pressures sufficiently low in order to avoid the influence of the space charge. Under these conditions the width of the N_2^+ ion peak is found to be less than 0.1 eV. It reflects essentially the thermal velocity distribution of the gas sample since the molecular ions have no kinetic-energy release.

To show that the peak structures in the ion-TOF spectra are indeed due to backward and forward ions, we have recorded ion-TOF spectra for different values of the extraction field. We have measured the Δt values for each ion class and deduced the ion-class energy with use of Eq. (1). We verify on Fig. 5 that the measured ion energies are indeed independent of the extraction field F (which provides an additional proof that space-charge effects are avoided). The overall relative uncertainty in the ion-energy measurements—including statistical errors—is found to be $\pm10\%$.

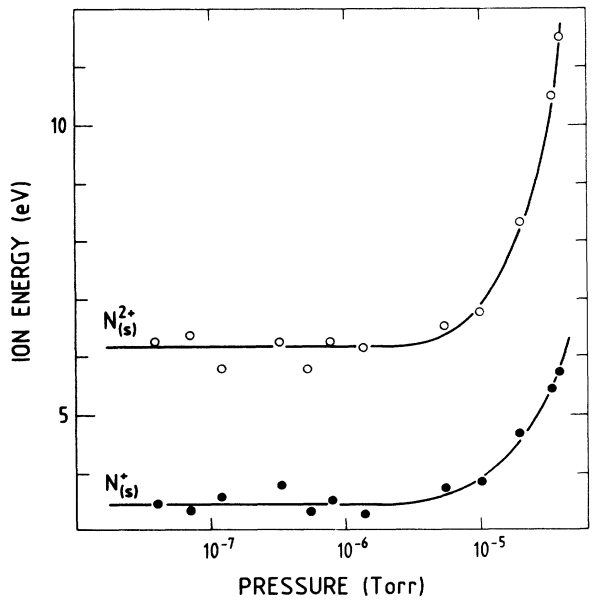

FIG. 4. Initial kinetic energies of slow N^+ and N^{2+} measured as a function of the operating pressure in the interaction chamber. The space-charge effects appear at 10^{-5} Torr and result in an increase of the ion energies.

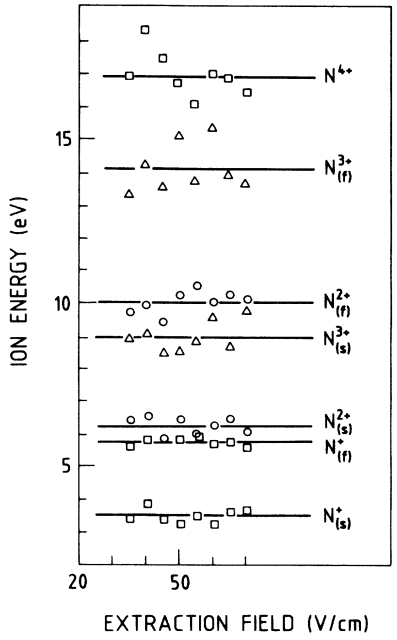

FIG. 5. Initial kinetic energies of the fragment ions measured vs the extraction field. The lines represent the average values of the ion energies. The vertical error bar is estimated to be 10% and the statistical error is inferior to 5%.

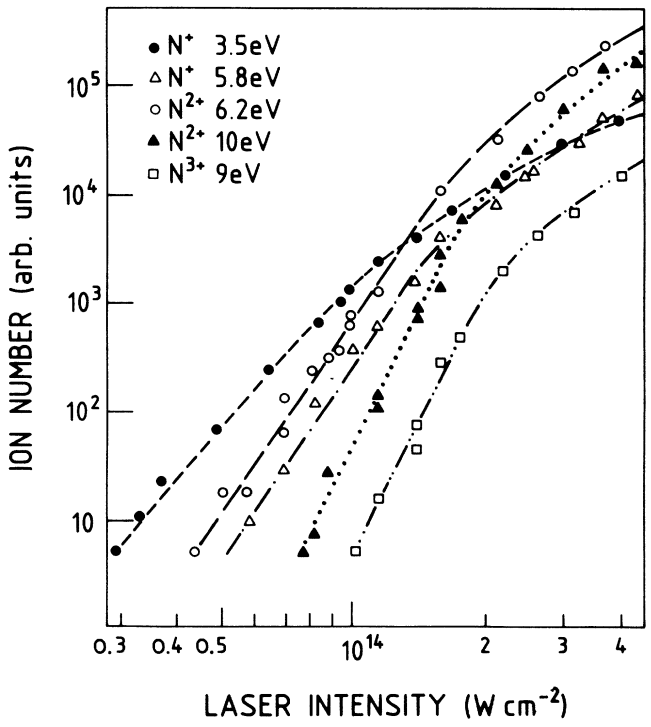

FIG. 6. Number of atomic ions vs the laser intensity at 610 nm. The N_2 pressure is varied from 10^{-7} to 10^{-5} Torr in order to keep a constant ion yield as the laser intensity is decreased.

The measurements of the initial kinetic energies of the fragments are the main, but not the only, means of investigation to identify the dissociation processes. In fact, two ion species issued from the same parent ion must exhibit the same dependence on the laser intensity. Therefore, the comparison of the ion-signal intensity dependences indicates if two peaks may be correlated or not. Figure 6 shows a log-log plot of the different ionic fragment signals as a function of the laser intensity. The N_2 signal being out of scale is not represented on the figure. To perform these measurements, we use the 150-mm focal length lens giving a larger interaction volume than the spheroparabolics lens. Under these conditions, the saturations of the different processes involved—which correspond to the depletion of the corresponding initial state—are only observed for large ion signals. Below saturation, the power dependence of the different ion classes is characterized by the power law k which is defined as

$$k=\partial\log_{10}(N_i)/\partial\log_{10}(I)\ , \tag{2}$$

where N_i is the number of ions at the laser intensity I. The interpretation of the k values depend on whether the interaction can be described as a multiphoton process or as a tunneling process, according to the values of Keldysh parameter γ (Ref. 20) defined as

$$\gamma=(E_i/1.87\times10^{-13}I\lambda^2)^{1/2}\ , \tag{3}$$

where the ionization potential E_i is expressed in eV, I in W/cm^2, and λ in μm.

In the multiphoton regime ($\gamma\gg1$), and in the absence of resonances, the power-law values represent the number of photons to be absorbed for ionization. This model should describe correctly the single ionization of N_2 at 610 nm and the experiment performed at 305 nm. For the other results obtained at 610 nm, the γ values are close to unity. In this intermediate regime, the interpretation of the power law is not so straightforward, the k values measured being usually much smaller than the number of photons necessary for ionization. The power laws measured in Fig. 6 as well as the kinetic energy values of the different ion species are summarized in Table I.

TABLE I. Initial kinetic energies and power laws of the different classes of ions observed at 610 nm.

	Initial energy (eV)	Power law (K)
N_2^+	0	6±1
N^+	3.5±0.4	4.9±0.4
	5.8±0.6	6.1±0.6
N^{2+}	6.2±0.7	6±0.5
	10±1.1	8.5±0.5
N^{3+}	9±1	8.3±1
	14.1±1.7	
N^{4+}	16.9±2	

B. Discussion

The results of Fig. 6 clearly indicate that the laser intensity is an essential parameter in the N_2 fragmentation processes. It thus appears convenient to discuss the results of Sec. III A by considering the sequence of events occurring during the laser-pulse raise time at the center of the focal spot. At the end of the discussion we will consider the effects of the spatial intensity distribution on the ion-population measurements.

(1) For intensities below 5×10^{13} W/cm^2 we essentially detect molecular N_2^+ ions. The formation of N_2^+ ions from the N_2 ground state requires the absorption of at least eight photons at 610 nm. The power law of the ion yield is found to be 6 ± 1, probably because of the occurrence of quasi resonances in the discrete spectrum of N_2. The saturation intensity is about 7×10^{13} W/cm^2.

(2) As far as the fragments are concerned, the 3.5-eV N^+ ions are predominant up to about 10^{14} W/cm^2. We exclude the formation of N^+ ions with such high energies by fragmentation of molecular ions N_2^+. The 3.5-eV N^+ fragments must then proceed from dissociative or quasibound states of N_2^{2+} according to

$$N_2^{2+}\rightarrow N^+ + N^+ + (7\pm0.8\ \text{eV})\ . \tag{4}$$

Indeed, the 3.5-eV measured energy is in good agreement with the previous results obtained at 600 nm with subpicosecond laser radiation.[11] It also confirms the energies obtained by different methods of excitation such as bombardment of N_2 by 1-MeV He^+ ions,[21] electron impact,[22–24] and synchrotron radiation.[25] If we assume that the double multiphoton ionization occurs at the equilibrium internuclear distance of N_2, then, within the Franck-Condon region, two low-lying quasibound states of N_2^{2+} dissociate into N^+ fragments with 3.5 ± 0.4 eV kinetic energies.[25,26] They are the $A\ ^3\Sigma_g^-$ and $b\ ^1\Pi_u$ states which correlate to the $N^+(^3P)+N^+(^3P)$ separated atom limit. Finally we note that the 3.5-eV N^+-ion yield saturates for relatively low number of ions revealing the existence of competing processes which tend to deplete the N_2^{2+} reservoir to form N_2^{3+}.

(3) The central peak between the N^+-ion peaks [Fig. 2(b)] appears at 10^{14} W/cm^2. It corresponds to zero-kinetic-energy ions, most probably metastable N_2^{2+} molecules. Above 10^{14} W/cm^2, the 5.8-eV N^+ and 6.2-eV N^{2+} populations become prominent. These two ion classes have very close initial kinetic energies and below 1.5×10^{14} W/cm^2 the two ion populations present the same dependence on the laser intensity (Fig. 6). Consequently, we assume that they arise from the dissociation of the same parent ion according to the reaction

$$N_2^{3+}\rightarrow N^{2+} + N^+ + (12\pm1.2\ \text{eV})\ , \tag{5}$$

the total energy being partitioned between the two fragments since their masses are equal. The N_2^{3+} ions cannot be created by vertical excitation from equilibrium internuclear separation of N_2. Otherwise, the Coulomb explosion of the molecule would lead to the creation of fragments with much greater energies than those measured. In fact, our results are consistent with the model proposed by Codling *et al.*[12] which assumes that the N_2^{3+} ions are formed by ionization of N_2^{2+} as the molecule dissociates. Then the molecular coupling is well represented by a coulombic repulsion between the two fragments. So, taking into account the total energy supplied to the fragments, we are able to identify the internuclear distance for which the ionization occurs, i.e., 2.4 Å.

From 1.5×10^{14} W/cm^2, the 6.2-eV N^{2+} signal increases more rapidly than the 5.8-eV N^+ signal. Two mechanisms may be responsible for this excess in the N^{2+} production. The first one is the subsequent ionization of the 5.8-eV N^+ ions following dissociation of N_2^{3+}. In the second one the N^{2+} ions are produced by dissociation of highly excited states of N_2^{2+} according to

$$N_2^{2+}\rightarrow N^{2+} + N + (12.4\pm1.4\ \text{eV})\ . \tag{6}$$

This charge asymmetric channel has been observed in soft-x-ray studies[27] and multiphoton experiments with 248-nm radiation at an intensity of 10^{16} W/cm^2.[10,28] The dissociation is then supposed to be slow enough to avoid the subsequent ionization of the neutral fragments. At 610 nm we have no experimental argument to privilege one or the other mechanism but at 305 nm, as we report in Sec. IV B, the latter is found to play the essential role in the production of N^{2+} fragments.

(4) For intensities higher than 2×10^{14} W/cm^2; the 10-eV N^{2+}-ion population becomes predominant indicating that the N_2^{3+} ionization rate increases to the detriment of its dissociation rate. Indeed, taking into account the relative ion abundances, the 10-eV N^{2+} peak cannot be correlated with any other peak and is generalized by the reaction

$$N_2^{4+}\rightarrow N^{2+} + N^{2+} + (20\pm2.2\ \text{eV})\ . \tag{7}$$

The energies of the fragments imply that the N_2^{3+} ionization into N_2^{4+} ion occurs at an internuclear distance of 3.6 Å.

In the same intensity range we detect a small peak of N^{3+} ions with an energy of 9 eV. This ion class could be correlated to part of the 10-eV N^{2+} ions involving the reaction $N_2^{5+}\rightarrow N^{3+}+N^{2+}+(19\pm2$ eV) generated by the ionization of the N_2^{4+} transient molecular ions. This process occurs necessarily at very large internuclear distance ($R>30$ Å) since there is no energy gain between the kinetic energies of the $N^{2+}+N^{2+}+(20\pm2.2$ eV) and $N^{3+}+N^{2+}+(19\pm2$ eV) channels. In that case, we consider that the N^{3+} ions are produced by the multiphoton ionization of N^{2+} fragments. This also explains the saturations of the two signals from about the same intensity.

(5) From 10^{15} W/cm^2, a group of N^{3+} ions with 14.1 ± 1.7 eV energy values is detected (Fig. 5) whereas no N^+ or N^{2+} ions with such a kinetic energy are detected. Therefore, they are assumed to come from the following dissociation process:

$$N_2^{6+}\rightarrow N^{3+} + N^{3+} + (28.2\pm3.4\ \text{eV})\ . \tag{8}$$

The absence of the channel $N_2^{5+}\rightarrow N^{2+}+N^{3+}$ implies that N_2^{6+} is formed by the quasicollective ejection of two electrons of N_2^{4+} at an internuclear distance of 8.8 Å.

This phenomenon can be related to the particularity of the molecular bonding at such a large internuclear separation. Indeed it consists in multiphoton ionization of two atomic ions mutually repelling rather than in collective emission of two electrons from a molecular ion.

Finally, at 5×10^{15} W/cm^2, we observe the presence of N^{4+} ions whose energies are found to be 16.9±2 eV. Due to the weakness of the N^{4+} population we cannot settle whether or not there exists a small component in the N^{3+} peak with an energy of 17 eV. Therefore the N^{4+} ions could arise from the dissociation of $N_2{}^{7+}$ or $N_2{}^{8+}$ molecular ions. By analogy with the preceding step, we assume that the N^{4+} ions more likely arise from a dissociation channel involving the formation of $N_2{}^{8+}$ from $N_2{}^{6+}$ at an internuclear distance of 18 Å according to

$$N_2{}^{8+}\rightarrow N^{4+}+N^{4+}+(33.8\pm4\text{ eV})\ . \quad (9)$$

In conclusion, as the laser pulse develops the dissociating molecular ion is sequentially stripped of its electrons at increasing internuclear distances (Fig. 7). Due to the higher order of the processes involved, as soon as the intensity required by a given ionization step is reached we consider that the ionization probability is equal to unity. Consequently, essentially N^{3+} and N^{4+} ions are formed at the center of the interaction volume. The intermediate reactions occur in outer parts of the interaction volume where the intensity is lower. For example, the 3.5-eV N^+ ions are created at the periphery of the interaction region in which the laser intensity is too low to strip another electron either from the molecular or from the atomic ions.

IV. STUDY AT 305 nm

A. Results

At a laser wavelength of 305 nm and a peak intensity of 3×10^{14} W/cm^2, we obtain the TOF ion-mass spectrum of N_2 represented on Fig. 8. Although the laser intensity range is similar to that investigated at 610 nm, the TOF spectrum is significantly different: (i) The fragmentation rate is here very important since the N^+-ion yield exceeds the $N_2{}^+$ one. (ii) We detect only two charge states of nitrogen fragments.

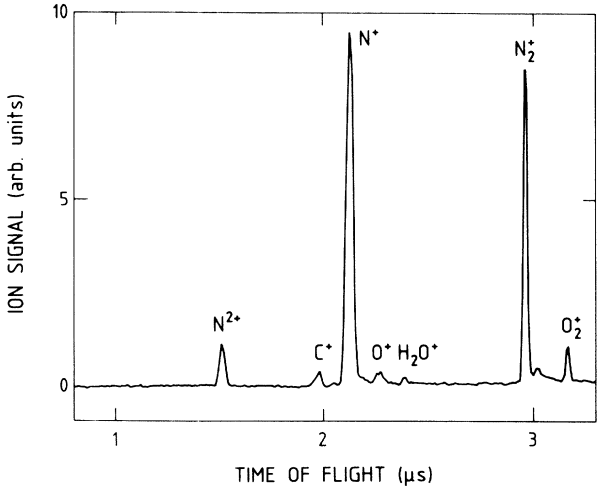

FIG. 8. TOF ion-mass spectrum of N_2 obtained at 3×10^{14} W/cm^2 using a 305-nm, 1.4 ps laser radiation. A 700-V-high voltage is applied along the 10-mm interaction chamber and the pressure is 8×10^{-6} Torr.

Figure 9 shows the TOF spectrum of the ionic fragments when the extraction field in the interaction chamber has been reduced to 50 V/cm. The choice of an operating pressure of 4×10^{-6} Torr is justified since we have verified (as on Fig. 4) that the effect of the space charge only appears at 10^{-4} Torr at 305 nm. We note that the N^+-ion signal is characterized by two energy classes as well as a central zero-kinetic-energy group. This latter is assumed to be related to the detection of metastable molecular ions whose lifetimes are of the order or greater than their corresponding time of flight.

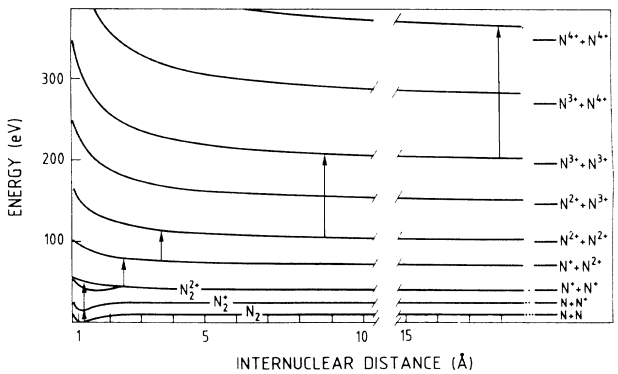

FIG. 7. Simplified potential-energy diagram of N_2 showing the different processes involved at 610 nm. From $N_2{}^{2+}$ the molecular dissociation is described by the coulombic repulsion between the two fragments.

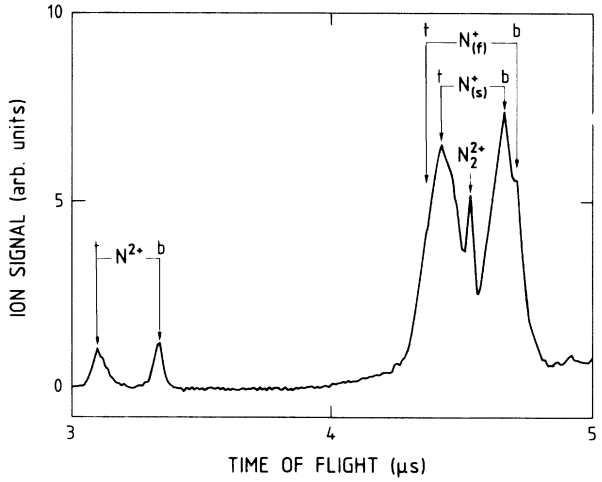

FIG. 9. TOF on mass spectrum of N_2 recorded at 3×10^{14} W/cm^2 and a pressure of 4×10^{-6} Torr. The extraction field is 40 V/cm.

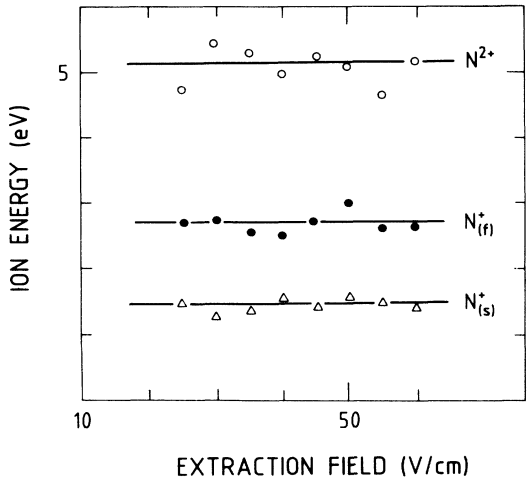

FIG. 10. Initial kinetic energies of N^+ and N^{2+} as a function of the extraction field. The lines indicate the average values of the measurements (the vertical error bar is about 10%).

Concerning the N^{2+} ions, only one energy class is detected. So as to determine the fragment initial energies, we have recorded several spectra associated with various extraction fields and indicated our results on Fig. 10.

We have also studied the variations of the ion signals versus the laser intensity (Fig. 11). Due to the difficulty in separating the two N^+-ion classes at low intensity, we have only plotted the variations of the slower N^+-ion population. It is interesting to note that the saturation effect appears on the N_2^+ and N^+ signals only above an intensity of 3×10^{14} W/cm^2. The experimental results (power laws and initial kinetic energies of the ions) are summarized in Table II.

B. Discussion

For laser intensities below 3×10^{14} W/cm^2 (Fig. 11), the ion spectrum is dominated by the N_2^+ peak whose

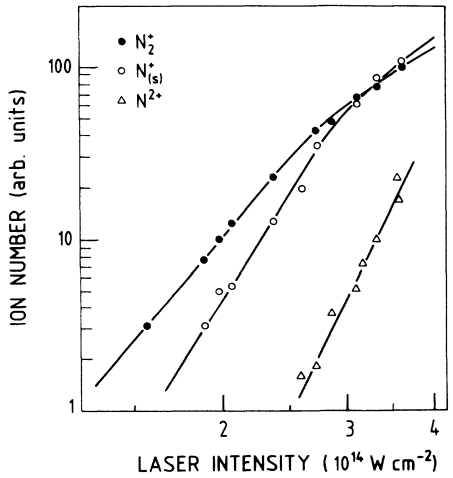

FIG. 11. Number of ions vs the laser intensity at 305 nm (the N_2 pressure is 8×10^{-6} Torr).

TABLE II. Initial kinetic energies and power laws of the different classes of ions observed at 305 nm.

	Initial energy (eV)	Power law (K)
N_2^+	0	4.8±0.3
N^+	1.45±0.2	6.4±0.4
	2.7 ±0.35	
N^{2+}	5.15±0.6	8.3±1

power law is found to be 4.8±0.5. This value is in agreement with the fact that a minimum of four photons is necessary to ionize the N_2 molecule. Above 3×10^{14} W/cm^2 the N_2^+ population is obviously depleted in favor of the N^+ populations.

The energies of the two classes of N^+ ions are found to be 1.45±0.2 eV and 2.7±0.35 eV. The preponderance of the N_2^+ population at low intensity implies that the N^+ ions cannot proceed from the multiphoton ionization of neutral fragments arising from the dissociation of N_2. The fragmentation mechanism thus occurs after the N_2^+ formation.

At sufficiently large internuclear distances, electronic states of doubly charged diatomic molecules dissociating to the single-charge atoms are mainly characterized by Coulomb repulsion of the atomic ions. The energies of the fragments are then expected to be greater than those of the slower N^+-ion class. In addition, the lowest electronics states of N_2^{2+} are about 4 eV above the $N^+ + N^+$ dissociation limit. Thus the 1.45-eV N^+ ions cannot be attributed to any fragmentation mechanism of the N_2^{2+} ions. Consequently, these ions are interpreted as resulting from the dissociation of N_2^+ molecules according to

$$N_2^+ \rightarrow N^+ + N + (2.9\pm0.4 \text{ eV}) . \quad (10)$$

This hypothesis is consistent with the power law of the N^+-ion yield—that is, 6.4±0.7—(Fig. 11) corresponding to a two-photon dissociation of N_2^+ following four-photon ionization.

The 2.7-eV N^+ ions are assumed to proceed from the dissociation of N_2^{2+} according to

$$N_2^{2+} \rightarrow N^+ + N^+ + (5.4\pm0.7 \text{ eV}) . \quad (11)$$

As at 610 nm, the N_2^{2+} are formed through a vertical transition from N_2 or N_2^+. The Franck-Condon overlaps for these processes are very favorable due to the close equilibrium internuclear distances of N_2, N_2^+, and N_2^{2+}. But the states of N_2^{2+} involved at 305 nm are situated below the $A\,^3\Sigma_g^-$ and the $b\,^1\Pi_u$ states involved at 610 nm since the kinetic-energy release at 305 nm (5.4 eV) is less than the kinetic-energy release at 610 nm (7 eV). Besides, the 2.7-eV measured energy is in agreement with experimental data related to electron-impact excitation[29] where N^+ ions are formed from the dissociation of low-lying quasibound states $a\,^3\Pi_u$ and $c\,^3\Sigma_u^+$, whose lifetimes lie in the 0.05–100 μs time scale. The lifetimes of these metastable states are much greater than the laser-pulse duration: the laser is switched off before the fragmentation of N_2^{2+} into $N^+ + N^+$ becomes significant. The main

consequence is the absence of a coulombic explosion of higher charge states of the molecule produced by the ionization of the dissociating N_2^{2+} ion as observed at 610 nm.

As shown on Fig. 9, a single class of N^{2+} ions is detected whose energy is found at 5.15 ± 0.6 eV (Fig. 10). These ions, as well as the metastable N_2^{2+} ions, become detectable for intensities above 3×10^{14} W/cm^2. They are not correlated with N^+ ions of the same initial energies and are thus generated by the reaction

$$N_2^{2+}\rightarrow N^{2+}+N+(10.3\pm1.2\text{ eV})\ . \tag{12}$$

The experimental appearance laser intensity of N^{2+} is close to the saturation intensity of the N^+ ions. Thus the N_2^{2+} excited states dissociating into $N^{2+}+N$ are most probably formed in a vertical transition from the lowest states $a\ ^3\Pi_u$ and $c\ ^3\Sigma_u^+$ of N_2^{2+} involved in the N^++N^+ fragmentation. These excited states are lying 64 eV above the N_2 ground state and could be triplet states close to the $A'\ ^3\Pi_u$ lying at 68.5 eV and observed in a recent experiment.[28] This result is consistent with previous measurements at 248 nm, where the N^{2+} energy spectrum exhibits a maximum in the 6–7-eV energy range associated with the $N^{2+}+N$ channel.[10] Considering that no N^+ peak with 5.15-eV energy is observed, we deduce that the neutral fragments are not subsequently ionized by the laser field. This implies that the dissociation process occurs after the extinction of the laser pulse. The possibility that the N^{2+} arise from the reaction $N_2^{4+}\rightarrow N^{2+}+N^{2+}+10.3$ eV is very unlikely because (i) this reaction cannot be initialized by the N^++N^+ as shown above; (ii) the $N_2^{3+}\rightarrow N^{2+}+N^+$ channel which would occur at a lower laser intensity is not observed.

As a conclusion at 305 nm, the lifetimes of the populated states of N_2^{2+} are too long to allow the ignition of the Coulomb explosion processes from the N^++N^+ repulsion as at 610 nm. As a consequence, we observe only vertical transitions up to the N_2^{2+} molecular ion which dissociates into N^++N^+ for the lowest metastable states and into $N^{2+}+N$ for the excited states.

V. CONCLUSION

Our results give new insight concerning the influence of the laser parameters on the multielectron dissociative ionization of diatomic molecules. By measuring the energy and the number of atomic fragments as a function of the laser intensity at 610 and 305 nm, we are able to identify the molecular response to the high-intensity laser field. In particular, the saturation and experimental appearance laser intensities allow to determine the dynamics of the excitation with respect to the time development of the laser pulse.

At 610 nm, the ionization steps occurs at increasing internuclear separations, i.e., during the dissociation process. The dissociation products have well-defined initial kinetic energies which implies that the ionization processes occur at given internuclear distances. In another work,[12] this phenomenon has been interpreted in terms of a simple field-ionization model. Assuming a pure coulombic repulsion between the atomic fragments, the entire sequence $N_2^{2+}\rightarrow N_2^{8+}$ is expected to occur within about 100 fs. However, the appearance intensities of the fragments measured in our experiment imply that the rise time of the laser pulse is too slow to account for such a rapid process. Consequently, the dissociation lifetimes of the N_2^{2+} levels populated must be sufficiently long (a few hundreds fs), otherwise the ionization steps would occur after the complete molecular dissociation, creating only multicharged fragments of identical energies. The N_2^{2+} states initializing the reactions at 610 nm are assumed to be the $A\ ^3\Sigma_g^-$ and/or $b\ ^1\Pi_u$ states. If the molecular structure plays an important role in the first stages of the ionization, the coulombic model accounts for the later stages (i.e., from the formation of N_2^{4+} for which both charge states and internuclear distance are sufficiently important). Finally in our interpretation, the dissociation of the N_2^{5+} and N_2^{7+} ions is not considered. The last ionization steps occur at such large internuclear distances that the transient molecular complex can be described as two atomic ions mutually repelling, the ionization of one ion rapidly following the ionization of the other one. At 305 nm, the lowest populated states of N_2^{2+} are found to be the $a\ ^3\Pi_u$ and $c\ ^3\Sigma_u^+$ electronic states dissociating into N^++N^+. The lifetimes of these metastable states are very long compared with the laser-pulse duration. As a consequence their dissociation is not yet effective when the laser pulse is switched off, and cannot allow the initialization of the Coulomb explosion of higher charge states of the molecule following the ionization of the dissociating N_2^{2+} ion. The $a\ ^3\Pi_u$ and $c\ ^3\Sigma_u^+$ states act as intermediate states for vertical subsequent transitions to electronic states situated 64 eV above the N_2 ground state and dissociating into $N^{2+}+N$.

The results at 610 and 305 nm indicate that the lifetimes of the different N_2^{2+} populated states at these two wavelengths are decisive quantities for initializing coulombic explosion processes. As a final remark, we point out that in the laser-intensity range investigated the energies of the fragments do not depend on the laser intensity. At 305 nm this result is not surprising since quasibound states with well-defined energies are responsible for the pattern fragmentation through vertical excitation. Conversely, at 610 nm the dissociation of the molecular ions is mainly due to repulsive coulombic states. We should then expect kinetic-energy releases showing large dispersion profiles which is obviously not the case. It should be pointed out that our measured energies are in good agreement with the results of Frasinsky *et al.*[11,12] whose laser-pulse duration is 0.6 ps, that is about three times smaller than in the present work. This fragmentation behavior which appears to be independent of the laser intensity and laser-pulse duration in the picosecond regime remains to be investigated in more detail.

ACKNOWLEDGMENTS

The authors are grateful to Pr. A. Giusti for fruitful discussions and to M. Bougeard, D. Fondant, E. Caprin, C. Robine, and A. Sanchez for their skilled technical assistance.

[1]C. Cohen-Tannoudji, and S. Reynaud, J. Phys. B **10**, 345 (1977).
[2]A. D. Bandrauk and N. Gélina, J. Chem. Phys. **86**, 5257 (1987).
[3]S-I. Chu, J. Chem. Phys. **75**, 2215 (1981).
[4]X. He, O. Atabek, and A. Giusti-Suzor, Phys. Rev. A **38**, 5586 (1988).
[5]A. Giusti-Suzor, X. He, O. Atabek, and F. H. Mies, Phys. Rev. Lett. **64**, 515 (1990).
[6]C. Cornaggia, D. Normand, J. Morellec, G. Mainfray, and C. Manus, Phys. Rev. A **34**, 207 (1986).
[7]D. Normand, C. Cornaggia, and J. Morellec, J. Phys. B **19**, 2881 (1986).
[8]J. W. J. Verschuur, L. D. Noordam, and H. B. Van Linden van den Heuvell, Phys. Rev. A **40**, 4383 (1989).
[9]J. Lavancier, D. Normand, C. Cornaggia, and J. Morellec, J. Phys. B **23**, 1839 (1990).
[10]K. Boyer, T. S. Luk, J. C. Solem, and C. K. Rhodes, Phys. Rev. A **39**, 1186 (1989).
[11]L. J. Frasinski, K. Codling, P. Hatherly, J. Barr, I. N. Ross, and W. T. Toner, Phys. Rev. Lett. **58**, 2424 (1987).
[12]K. Codling, L. J. Frasinski, and P. A. Hatherly, J. Phys. B **22**, L321 (1989).
[13]D. S. Bethune, Appl. Opt. **20**, 1897 (1981).
[14]A. Migus, C. V. Shank, E. P. Ippen, and R. L. Fork, IEEE J. Quantum Electron **QE-18**, 101 (1982).
[15]C. Kolmeder, W. Zinth, and W. Kaiser, Opt. Commmun. **30**, 435 (1979).
[16]L. A. Lompré, G. Mainfray, and J. Thebault, Rev. Phys. Appl. **17**, 21 (1982).
[17]W. C. Wiley and I. H. Mclaren, Rev. Sci. Instrum. **26**, 1150 (1955).
[18]M. Richard-Viard, O. Dutuit, M. Lavollée, T. Govers, P. M. Guyon, and J. Durup, J. Chem. Phys. **82**, 4054 (1985).
[19]B. Schram, A. Boerboom, W. Kleine and J. Kistemaker, *Proceedings of the Seventh International Conference on Phenomena in Ionized Gases, Belgrade, 1965,* edited by B. Perovic and D. Tosić (Gradjevinska Knjiga, Belgrade, 1966).
[20]L. V. Keldysh, Zh. Eksp. Teor. Fiz. **47**, 1945 (1964) [Sov. Phys.—JETP **20**, 1307 (1965)].
[21]A. K. Edwards and R. M. Wood, J. Chem. Phys. **76**, 2938 (1982).
[22]B. Brehm, and G. De Frehatnes, Int. J. Mass Spectrom. Ion, Phys. **26**, 251 (1978).
[23]P. C. Cosby, R. Moller, and H. Helm, Phys. Rev. A **28**, 766 (1983).
[24]F. Feldmeier, H. Durchholz, and A. Hofmann, J. Chem. Phys. **79**, 3789 (1983).
[25]M. J. Besnard, L. Hellner, G. Dujardin, and D. Winkoun, J. Chem. Phys. **88**, 1732 (1988).
[26]R. W. Wetmore, and R. K. Boyd, J. Phys. Chem. **90**, 5540 (1986).
[27]W. Eberhardt, E. W. Plummer, I.-W. Lyo, R. Carr, and W. K. Ford, Phys. Rev. Lett. **58**, 207 (1987).
[28]G. Gibson, T. S. Luk, A. McPherson, K. Boyer, and C. K. Rhodes, Phys. Rev. A **40**, 2378 (1989).
[29]J. M. Curtis, and R. K. Boyd, J. Chem. Phys. **81**, 2991 (1984).